

Effect of Nano-Silica Fillers on Surface Morphology and Mechanical Properties of Polymer-Silica Composites

Li-Piin Sung,¹ Dongmei Zhe¹, Aaron M. Forster¹, Peter Krommenhoek¹, Nancy J. Lin², and Sheng Lin-Gibson²

¹Materials and Construction Research Division, Building and Fire Research Laboratory, National Institute of Standards and Technology, Gaithersburg, MD 20899

²Polymers Division, Materials and Science Engineering Laboratory, National Institute of Standards and Technology, Gaithersburg, MD 20899

INTRODUCTION

Incorporating metal-oxide nanoparticles such as nano-alumina and nano-silica into polymeric coatings to enhance the mechanical durability has become a trend in the current anti-scratch and mar technologies [1]. Recent results [1-2] have shown promising results in the automotive coatings and other thin film coating applications. Other research efforts [3-4] have been focused on the effect on nanofillers on the materials properties of complex systems such as nanocomposites. In these systems, the surface properties may be very different from the bulk properties, the dispersion of the nanofillers and overall microstructure may influence the final properties. In this paper, we investigate a quantitative study on the effect of nano-silica on the surface morphology and mechanical properties on two-dimensional (2D) gradient polymer-silica composite samples varied in chemical composition (e.g., filler size/concentration). A combination of techniques including nanoindentation and laser scanning confocal microscopy was utilized to measure surface modulus and roughness, and map scratch damage patterns. Preliminary results show the addition of nano-silica reduces surface roughness, increases modulus and hardness, and improves scratch resistance of the polymer-silica composite systems.

EXPERIMENTAL[#]

Materials. The polymer matrix was a monomer system consisting of binary mixtures of 2,2-Bis(4-(2-hydroxy-3-methacryloxypropoxy)phenyl)propane dimethacrylate (BisGMA) and triethylene glycol dimethacrylate (TEGDMA). Resins BisGMA and TEGDMA were obtained from Esstech Inc. Photoinitiator system components, camphorquinone (CQ) and ethyl 4-*N,N*-dimethylaminobenzoate (4E), were purchased from Aldrich Corp. Two types of fillers were used. The micro-filler (SP 345 silane glass filler; SG, 0.70 μm average diameter) and the nanofiller (fumed amorphous silica filler, OX50, 0.04 μm average diameter) were provided by the L.D. Caulk Company. Methacryloxypropyltrimethoxysilane (MPTMS) and *n*-octadecyltrimethoxysilane (OTMS) were purchased from Gelest, Inc.

Composite Preparation. Gradient samples with variations in filler composition (type and content) and irradiation along orthogonal axes were fabricated (see Figure 1). BisGMA and TEGDMA (mass ratio = 50:50) were activated for blue light photopolymerization with 0.2 % CQ and 0.8 % 4E (by mass) and stored in the dark until use. The SG and OX50 fillers were mixed into the activated resin following the formulations shown in Figure 1b. In this report, the mass % of the resin is 35 % for all compositions. The 2D specimens consisted of a discrete array in composite formulation (individual stripes) along one axis with an orthogonal, gradient in methacrylate conversion. The specimens were fabricated and by adapting procedures previously used for specimens of unfilled polymers [7]. The conversion gradients were generated using the same polymerization protocol used previously [5-7], and the final degree of conversion (DC) measured by Near Infrared Radiation (NIR) spectroscopy. A notch was made across

the DC gradient at the high conversion end and defined as the zero position for subsequent measurements.

NIR Spectroscopy. Transmission NIR spectroscopy was performed using a Nicolet Magna 550 FTIR spectrometer (Madison, WI) configured with a white light source, a CaF_2 beam splitter, and an InSb detector. The NIR spectra in the region of 7000 cm^{-1} to 4000 cm^{-1} were acquired from 32 averaged scans at 6 cm^{-1} resolution. The NIR beam was placed at discrete locations along the gradient sample to measure DC. DC was quantified as 1 minus the ratio of the residual methacrylate C=C stretch (4743 cm^{-1}) peak height in the polymerized sample to the same peak in the uncured composite paste [6]. In addition, each peak was normalized to the aromatic peak height (4623 cm^{-1}) from the same sample. Conversion measurements were collected from zero position to 50 mm at 10 mm intervals. The relative uncertainty associated with the NIR measurements is 3 %.

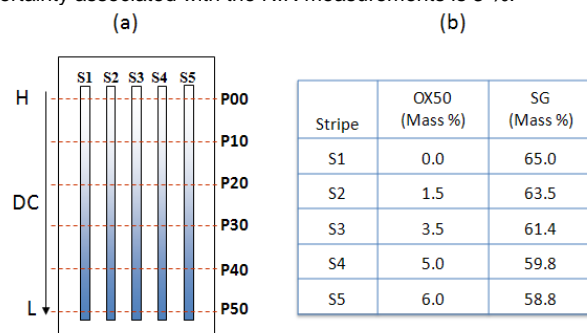


Figure 1. (a) Schematic of 2D gradient samples; (b) type and content of filler composition in each strip, the mass % of resin is 35 %.

Surface Mechanical Measurements and Scratch test. Surface mechanical properties of each composite strip was measured using a MTS XP nanoindenter with a 10 micron radius 45° semi-apical angle diamond cone indenter in a continuous stiffness mode and with a constant indentation strain rate of 0.05 s^{-1} . This stiffness was used to calculate the elastic modulus of the sample [8] using a Poisson's ratio of 0.35, a value found to be representative for polymer composites. The modulus and hardness were determined as the average value obtained over a depth ranging from 1000 nm to 4000 nm. The hardness to modulus ratio (H/E) was calculated from these averages. Mechanical data were collected and reported over a 50 mm length at 10 mm intervals beginning at the zero position (P00) for each composition. Three indents were measured at each location. The standard uncertainty associated with the nanoindentation measurements is 5 %.

The same indenter was used to scratch the surface of the gradient polymer composites. The scratch test method and measurement protocol used in this study can be found in [9]. The surface of each composite was scratched parallel to the conversion gradient and within 1 mm of each indent location using the same indenter. A progressive-load scratch method was used to produce three 400 μm scratches parallel to the curing gradient from 0 mm to 50 mm at 10 mm intervals. All scratch tests are at a fixed velocity of 10 $\mu\text{m/s}$ with scratch loads progressively increasing linearly from nominally 20 μN to approximately 50 mN. Penetration depth (scratch and residual), pile-up height, and percentage of recovery for various nanofiller concentrations are reported.

Surface Morphology Characterization. A Zeiss model LSM510 reflection laser scanning confocal microscope (LSCM) was employed to characterize surface morphology (topographic profile) and scratch damage. A detailed description of LSCM measurements can be found elsewhere [9,10]. The laser wavelength used in this study was 543 nm. LSCM images presented in this paper are 2D intensity projections (an image formed by summing the stack of images over the z direction, (512 pixel x 512 pixel) of the composite surface. The 2D intensity projection images are effectively the sum of all the light scattered by different layers of the composites, as far into the composites as light is able to penetrate. The pixel intensity level represents the total amount of back-scattered light. Darker areas represent regions scattering less

[#] Certain instruments or materials are identified in this paper in order to adequately specify experimental details. In no case does it imply endorsement by NIST or imply that it is necessarily the best product for the experimental procedure.

light than lighter colored areas. The scratch width was defined as the peak-to-peak distance perpendicular to the scratch length.

RESULTS AND DISCUSSION

A schematic of the 2D array gradient polymer-silica composite samples varied in chemical composition (e.g., filler size/concentration) and DC on the orthogonal axes is shown in Figure 1a. Chemical compositions (S1 to S5) were kept discrete and were based on the same resin system of same mass fraction (35 mass %), while the filler size (macrofiller and/or nanofiller) and mass fraction were varied to investigate their effects on material properties. Each composition was then polymerized to form a gradient in DC (high DC end at 0 mm). As will be discussed, the array sample was successfully used to identify significant differences in surface roughness and mechanical properties as a function of filler type/content and DC.

Figure 2a shows DC for the gradient samples. With increasing nanofiller content, the overall DC values increase in all positions. Noticeable changes (still less than 0.02 in DC) were observed between S1 and S2 strips. S3 thru S5 were statistically identical for any given position along the conversion gradient. These results show the nanofiller content (> 3.5 mass %) does not strongly affect the DC for the formulations described within this study. Note that the composites examined in this study are largely (or exclusively) filled with micron size fillers. This result suggests that the filler fraction does not affect the conversion in composites filled with micron size fillers. Given that the differences were small between S1 and the other compositions, we chose to treat DC as equivalent for all compositions at any given position along the DC gradient, and material properties were compared as a function of position from here on.

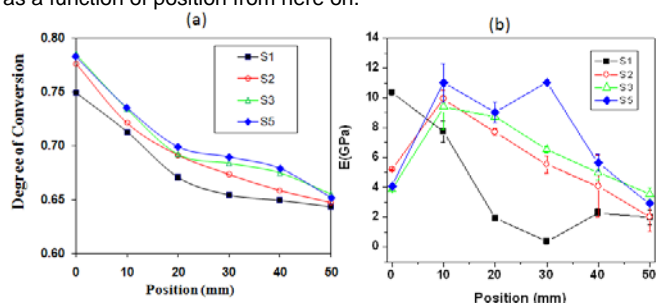


Figure 2. (a) DC and (b) E as a function of sample position for each strip. The estimated uncertainty is 2 % in the DC data. Error bars in (b) represent one standard deviation. Lines are drawn to aid the reader's eyes.

2D LSCM projection images of the surface roughness (not shown here) revealed a generally smooth surface at high DC that became progressively rougher with decreasing DC. The same trend was observed for all compositions and using two different microscope objectives (areas of 1840 μm x 1840 μm and 184 μm x 184 μm). The RMS surface roughness measured at area of 184 μm x 184 μm . At P00-P10 positions, all surfaces look smooth for all strips and roughness values increase as DC decreases. Noticeably, with only 1.5 mass % of nanofillers (see Strip S2); the roughness values reduce dramatically at position P20, and decrease furthermore as increasing nanofiller contents. Similar effects were also observed in surface mechanical property (elastic modulus (E) and hardness (H)) measurements. The E value (Figure 2b) decreases as decreasing DC for all compositions. Again with 1.5 mass % of nanofillers, the E value increases dramatically especially in the position between P10 to P40. Similar trends were in the H data (not shown here) and the ratio of H/E reflects the general trends.

The H/E ratio is a qualitative approach for estimating the scratch performance of materials and coatings, with a higher H/E indicating improved scratch resistance and wear [11]. The highest H/E ratio occurred in the region of highest DC and was due to the increase in hardness, which tends to outpace the increase in modulus as DC increased. For all compositions, an increased H/E ratio was observed as DC increased, indicating that the materials became more resistant

to plastic deformation at higher DCs. S2 thru S5 showed qualitatively similar results at each position. S1 has the lowest H/E ratio and indicates the worst scratch resistance. These results are consistent with the scratch test results. Figure 3 shows the scratch damage at a scratch load of 49 mN for three nanofiller contents (0 %, 1.5 %, and 3.5 %) at the position P30. The damage such as scratch width and depth decreases as nanofiller content increases.

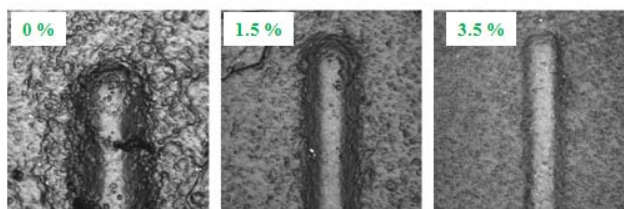


Figure 3. LSCM images of scratch damage at a scratch load of 49 mN at P30 for three nanofiller contents (0 %, 1.5 %, and 3.5 %). Each image size is 64 μm x 64 μm .

CONCLUDING REMARK

Effect of Nanofillers on the surface morphology and mechanical properties of 2D gradients polymer-silica composites have been investigated by various techniques. Overall, the results suggest that filler mass fraction, the presence of nanofiller, and the degree of conversion work in concert to affect the surface properties, mechanical properties.

REFERENCES

1. ACS Symposium Series1008: Nanotechnology Applications in Coatings, Eds: Fernando, R.H.; Sung, L.; ACS/Oxford Press, Washington DC, **2009**.
2. Sung, L.; Comer, J.; Forster, A.M.; Hu, H.; Floryancic, B.; Brickweg, L.; and Fernando, R.H.; *J. Coat. Technol. and Res.*, **2008**, 5(4) 419.
3. Garcés, J.M.; Moll, D.J.; Bicerano, J.; Fibiger, R.; McLeod, D.G.; *Advanced Materials* **2000**, 12, 1835.
4. Wetzel, B.; Hauptert, F.; Friedrich, K.; Zhang, M.Q.; Rong, M.Z. *Polymer Engineering and Science* **2004**, 42, 1919.
5. Lin, N.J.; Drzal, P.L.; Lin-Gibson S. *Dental Materials* **2007**, 23, 1211.
6. Lin-Gibson, S.; Landis, F.A.; Drzal, P.L. *Biomaterials* **2006**, 27, 1711.
7. Lin-Gibson, S.; Sung, L.; Forster, A.M.; Hu, H.; Lin, N.J. *Acta Biomaterialia* **2009**, DOI.
8. VanLandingHam, M.R. *Journal of Research of the National Institute of Standards and Technology* **2003**; 108, 249.
9. Sung, L.P.; Drzal, P.L.; VanLandingham, M.R.; et al. *JCT research* **2005**, 8, 583.
10. Sung, L.; Jasmin, J.; Gu, X.; Nguyen, T.; and Martin, J.W. *JCT Research* **2004**, 1, 267.
11. Gauthier, C.; Durier, A.L.; Fond, C.; Schirrer, R. *Tribology International* **2006**, 39, 88.